Proceedings, Bulk Metallic Glasses Conference, Singapore, September 24-28, 2000

Anomalous small-angle x-ray scattering studies of phase separation in bulk amorphous $Zr_{52.5}Ti_5Cu_{17.9}Ni_{14.6}Al_{10}$

T. C. Hufnagel and X. Gu

Department of Materials Science and Engineering,

Johns Hopkins University, Baltimore, Maryland 21218

A. Munkholm

Chemistry Division, Argonne National Laboratory,

Argonne, Illinois 60439

Abstract

We have perfomed differential anomalous small-angle x-ray scattering (ASAXS) experiments on samples of bulk amorphous $Zr_{52.5}Ti_5Cu_{17.9}Ni_{14.6}Al_{10}$ annealed in the supercooled liquid region. We observe the development of strong small-angle scattering, associated with phase separation on the nanometer scale in the supercooled liquid. Analysis of the Zr-edge ASAXS data reveals that this phase separation is largely due to a redistribution of Zr. Continued anneal-

DISCLAIMER

ing results in the nucleation and growth of Zr-rich crystalline intermetallic phases.

Introduction

Recently, it has been established that several Zr-based bulk glass-forming alloys undergo phase separation by spinodal decomposition upon annealing, prior to crystallization. In $Zr_{41.2}Ti_{13.8}Cu_{12.5}Ni_{10}Be_{22.5}$, for instance, small-angle neutron scattering (SANS)[1] and atom-probe field-ion microscopy [2, 3] have revealed phase separation on nanometer length scales in the supercooled liquid region. Other alloys, such as $Zr_{52.5}Ti_5Cu_{17.9}Ni_{14.6}Al_{10}$ and $Zr_{57}Nb_5Cu_{15.4}Ni_{12.6}Al_{10}$, show similar behavior, which appears to be correlated with the excellent glass-forming ability of these alloys [4]. Not all Zr-based metallic glasses, however, undergo phase separation; $Zr_{46.8}Ti_{8.2}Cu_{7.5}Ni_{10}Be_{27.5}$ is an example, which may explain why its glass-forming ability is not as good as some of the other Zr-based alloys [5].

It is apparent from these studies that phase separation in the undercooled liquid can have a significant effect on the crystallization of Zr-based bulk glass-forming alloys. In such multicomponent systems, however, the kinetics

of phase separation and crystallization can be quite complex. For instance, multiple miscibility gaps may exist, occurring at different temperatures and with different chemical compositions of the phase-separated regions. Furthermore, it is an open question as to whether phase separation by spinodal decomposition is also a common feature of multicomponent glass-forming alloy systems other than those based on zirconium.

In order to better understand the details of phase separation and crystallization in $Zr_{52.5}Ti_5Cu_{17.9}Ni_{14.6}Al_{10}$, we have performed small-angle x-ray scattering and anomalous small-angle x-ray scattering (ASAXS) on samples annealed at temperatures near the glass transition. We observe the development of a maximum in the SAXS and ASAXS scattering intensity, indicating the development of phase separation on the nanometer scale. ASAXS observations performed near the Zr-K absorption edge reveal that the distribution of Zr is homogeneous in the as-cast samples, but becomes increasingly inhomogeneous with increasing annealing time. These observations correlate well with recent observations of phase separation in $Zr_{52.5}Ti_5Cu_{17.9}Ni_{14.6}Al_{10}$ by SANS [4], indicating the scattering maximum in those studies was also due to a phase separation involving zirconium.

Experimental Procedure

The metallic glass samples used in this study were prepared by arc melting master alloy ingots of the desired composition from high purity elemental starting materials under a purified Ar atmosphere. $Zr_{52.5}Ti_5Cu_{17.9}Ni_{14.6}Al_{10}$ and related alloys that do not contain beryllium are quite sensitive to contamination (particularly by oxygen); therefore, we find it necessary to remove surface contamination from the as-received starting materials by either chemical etching or mechanical polishing. The master alloy ingots were then cast into a copper mold to produce 3 mm diameter cylindrical rods using a suction-casting method that is described in more detail in Reference [6]. The resulting rods are fully amorphous (as determined by transmission electron microscopy), except for a thin ($\sim$ 5-10 μm) thick shell of crystalline material where the ingot was in contact with the mold wall. The oxygen content of several representative samples was measured using Leco analysis; in every case, the oxygen contamination level was less than 100 ppm, indicating the effectiveness of the steps taken to reduce contamination. The samples were annealed under Ar in a differential scanning calorimeter, following which thin specimens suitable for SAXS were prepared by sectioning

and mechanical polishing.

We performed the SAXS observations on beamline 12-ID of the Advanced Photon Source at Argonne National Laboratory; the design and operation characteristics of the SAXS instrument are described in detail in Reference [7]. Scattering experiments were conducted at x-ray energies near the Zr-K, Cu-K, and Ni-K absorption edges, which occur at 17998 eV, 8979 eV, and 8333 eV, respectively. Only the Zr-edge results are reported here. The data were normalized by comparison to the scattering from a polyethylene sample measured under identical experimental conditions.

Results

Figure 1(a) shows a differential scanning calorimetry trace from a sample heated at 10 K/min. The glass transition occurs at 685 K, with the onset of crystallization at about 720 K. There are two distinct but overlapping exothermic peaks in the DSC trace; the physical processes causing these two peaks can be examined separately by isothermal annealing at a temperature below 720 K (Figure 1(b)). Although we have not examined the nature of the structural changes associated with the first exotherm in detail, in closely

related alloys this exotherm is associated with the formation of nanometer-scale quasicrystalline precipitates [8]. It is likely that a similar process occurs in $Zr_{52.5}Ti_5Cu_{17.9}Ni_{14.6}Al_{10}$.

Structural changes during annealing are illustrated by the x-ray diffraction scans in Figure 2. The as-cast specimens (Fig. 2(a)) show a broad scattering feature characteristic of an amorphous material. Annealing for 90 min at 705 K results in the nucleation crystalline intermetallic phases, principally Zr_2Ni and Zr_2Cu (Fig. 2(b)). The x-ray diffraction peaks are weak and broad, indicating that the crystallites are quite small. Upon annealing to 973 K, the intermetallic crystals grow significantly, causing the x-ray diffraction peaks to become more distinct (and more amenable to identification).

For the small-angle scattering studies, we examined samples in the as-cast state, and annealed at several temperatures below the onset of crystallization in the DSC scan. Figure 3 shows the evolution of the small-angle scattering intensity (at an x-ray energy of 17898 eV) for an as-cast samples and samples annealed for various durations at 705 K. The as-cast sample shows essentially no small-angle scattering, indicating that the material is chemically homogeneous (on nanometer length scales). Upon annealing, a prominent maximum in the scattered intensity develops, providing evidence for the development of

phase separation. With increased annealing time, the intensity of scattering increases and the position of the maximum shifts to smaller scattering angle, consistent with a spinodal decomposition mechanism.

The SAXS patterns in Fig. 3 clearly indicate the development of phase separation upon annealing. They are not, however, capable of directly revealing which elements are involved in the phase separation or the chemical composition of the phase separation products. This is because x-ray scattering is fundamentally sensitive to fluctuations in electron density, not composition. However, it is possible to extract species-specific information from x-ray scattering by using x-ray energies near an absorption edge of an element of interest; this technique is called anomalous scattering [9]. Near the Zr-K absorption edge, the Zr scattering factor changes significantly, while those of the other elements remains essentially unchanged. As a result, any change in scattered intensity with x-ray energy in this energy region is to a reasonable approximation due only scattering events involving Zr atoms. Thus, the *difference* in small-angle scattering between measurements made at two energies below the Zr absorption edge is sensitive to the distribution of Zr in the sample, without complicating contributions from other elements.

ASAXS observations from the samples annealed at 705 K are shown in

Figure 4, which may be compared with Figure 3. The general nature of the evolution of the SAXS and Zr-edge ASAXS are quite similar, demonstrating that the increase in scattered intensity observed in Figure 3 is due to the development of nanometer-scale regions enriched (or depleted) in Zr. On the basis of these observations, one cannot rule out the possibility that the phase separation also involves other elements (Cu and Ni in particular). Indeed, the fact that the final crystallization products include Zr_2Ni and Zr_2Cu indicates that some redistribution of Cu and Ni must occur. This possibility could be examined by ASAXS measurements at the relevant absorption edges.

One question that remains to be answered is the relationship between the phase separation and the nucleation and growth of nanometer-scale crystalline precipitates. A likely possibility is that phase separation occurs by spinodal decomposition, and that the resulting decomposed phases are more favorable than the homogeneous alloy for nucleation and growth of the crystalline phases. If this is the case, one might also expect to see a separate composition redistribution at longer times, associated with the development of concentration gradients due to nucleation and growth of the crystalline phases. Whether or not this is observable depends in part on the composition of the decomposed amorphous phases compared to the growing crystalline

phases.

Summary

We have observed phase separation in bulk amorphous $Zr_{52.5}Ti_5Cu_{17.9}Ni_{14.6}Al_{10}$ that occurs during annealing in the supercooled liquid state. Anomalous small-angle x-ray scattering reveals that this phase separation involves a redistribution of Zr on the nanometer length scale. Continued annealing results in the nucleation and growth of crystalline intermetallic phases, suggesting that nucleation of these phases is more favorable in the decomposed phases than in the parent alloy. Phase separation prior to crystallization appears to be a common feature of Zr-based bulk amorphous alloys with good glass-forming characteristics.

Acknowledgements

We thank S. Seifert, R. E. Winans, A. Stux, and R. T. Ott for assistance in collecting the small-angle scattering data. T. C. Hufnagel gratefully acknowledges support for the small-angle scattering experiments from the U.S.

Department of Energy, Office of Basic Energy Sciences under grant DE-FG02-98ER45699. X. Gu acknowledges suppport for sample preparation, DSC, and x-ray diffraction work from the U. S. Army Research Office under grant DAAG55-98-1-0487. Use of the Advanced Photon Source was supported by the U. S. Department of Energy, Basic Energy Sciences, Office of Science, under Contract No. W-31-109-Eng-38.

References

[1] S. Schneider, P. Thiyagarajan, and W.L. Johnson. Formation of nanocrystals based on decomposition in the amorphous $Zr_{41.2}Ti_{13.8}Cu_{12.5}Ni_{10}Be_{22.5}$ alloy. *Appl. Phys. Lett.*, 68:493–495, 1996.

[2] R. Busch, S. Schneider, A. Peker, and W.L. Johnson. Decomposition and primary crystallization in undercooled $Zr_{41.2}Ti_{13.8}Cu_{12.5}Ni_{10.0}Be_{22.5}$ melts. *Appl. Phys. Lett.*, 67:1544–1546, 1995.

[3] M.-P. Macht, N. Wanderka, A. Wiedenmann, H. Wollenberger, Q. Wei, H.J. Fecht, and S.G. Klose. Decomposition of the supercooled liquid

of the bulk amorphous alloy $Zr_{41}Ti_{14}Cu_{12.5}Ni_{10}Be_{22.5}$. *Mat. Sci. Forum*, 225-227:65–70, 1996.

[4] J. F. Löffler, S. Bossuyt, S. G. Glade, W. L. Johnson, W. Wagner, and P. Thiyagarajan. Crystallization of bulk amorphous Zr-Ti(Nb)-Cu-Ni-Al. *Appl. Phys. Lett.*, 77:525–527, 2000.

[5] J. F. Löffler, P. Thiyagarajan, and W. L. Johnson. Concentration and temperature dependence of decomposition in supercooled liquid alloys. *J. Appl. Cryst.*, 33:500–503, 2000.

[6] X. Gu, L. Q. Xing, and T. C. Hufnagel. Preparation and glass-forming ability of bulk metallic glass $(Hf_xZr_{1-x})_{52.5}Cu_{17.9}Ni_{14.6}Al_{10}Ti_5$. Submitted to *J. Non-Cryst. Sol.*, 2000.

[7] S. Seifert, R. E. Winans, D. M. Tiede, and P. Thiyagarajan. Design and performance of a ASAXS instrument at the Advanced Photon Source. *J. Appl. Cryst.*, 33:782–784, 2000.

[8] L. Q. Xing, T. C. Hufnagel, J. Eckert, W. Löser, and L. Schultz. Relation between short-range order and crystallization behavior in Zr-based amorphous alloys. *Appl. Phys. Lett.*, 77:1970–1972, 2000.

[9] G. Materlik, C. J. Sparks, and K. Fischer, editor. *Resonant Anomalous X-ray Scattering: Theory and Applications.* North-Holland, 1994.

Figure Captions

1. Calorimetry results from amorphous $Zr_{52.5}Ti_5Cu_{17.9}Ni_{14.6}Al_{10}$. (a) Differential scanning calorimetry at a heating rate of 10 K/min shows a glass transition at 685 K followed by two exotherms corresponding to crystallization. (b) Isothermal annealing at 705 K shows the two isotherms from (a) as separate peaks.

2. X-ray diffraction patterns (Cu Kα radiation) from (a) an as-cast sample, (b) a sample annealed 90 min at 705 K, and (c) a sample heated to 973 K. The peak near 50° is from the sample holder. Note the lack of crystalline reflections in the as-cast sample, and the development of crystalline peaks due to intermetallic phases upon annealing.

3. SAXS patterns taken at 17898 eV as a function of annealing time at 705 K for amorphous $Zr_{52.5}Ti_5Cu_{17.9}Ni_{14.6}Al_{10}$. The as-cast sample shows essentially no small-angle scattering, indicating that it is chemically homogeneous. Upon annealing, a pronounced maximum in the SAXS pattern develops due to phase separation.

4. Zr-K absorption edge ASAXS observations (determined from the difference in scattering between two measurements at energies 10 eV and 100 eV

below the absorption edge) for the same samples as in Figure 3. These ASAXS patterns are only sensitive to the distribution of Zr; the fact that a scattering maximum develops indicates that the phase separation observed in Figure 3 is largely the result of Zr redistribution.

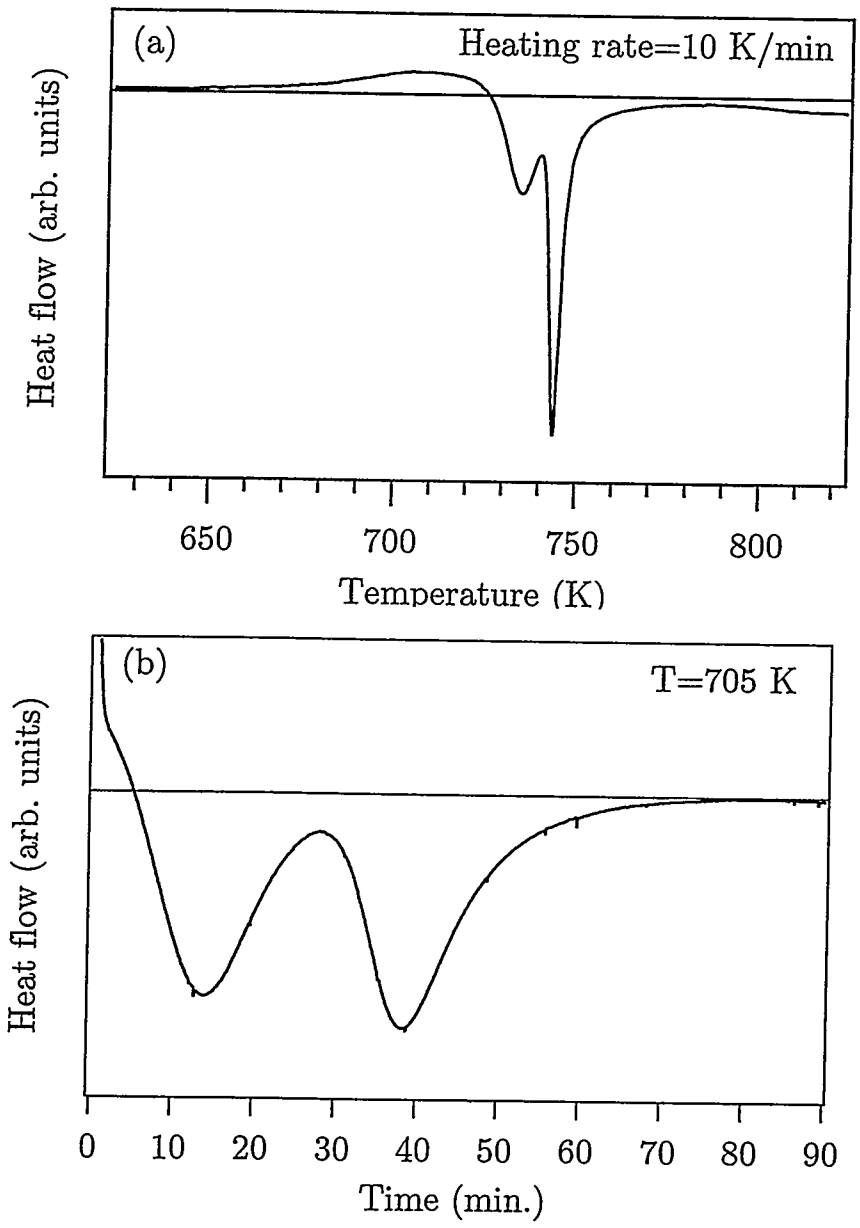
(a)
Heating rate=10 K/min
Heat flow (arb. units)
650
700
750
800
Temperature (K)
(b)
T=705 K
Heat flow (arb. units)
0
10
20
30
40
50
60
70
80
90
Time (min.)

Figure 1:

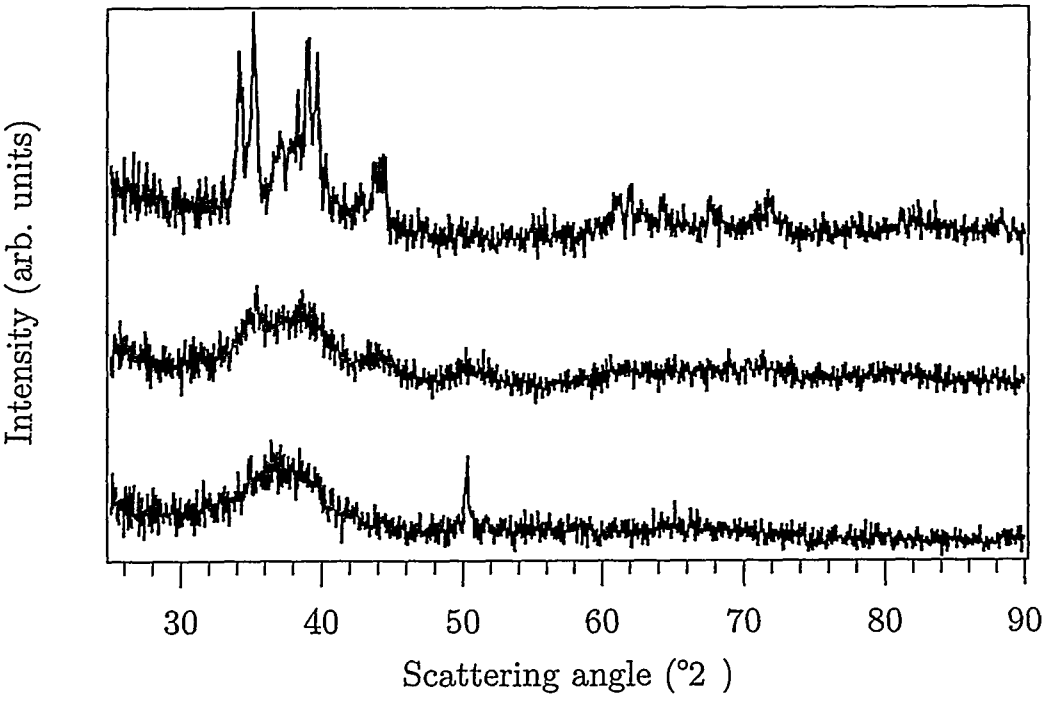

Figure 2:

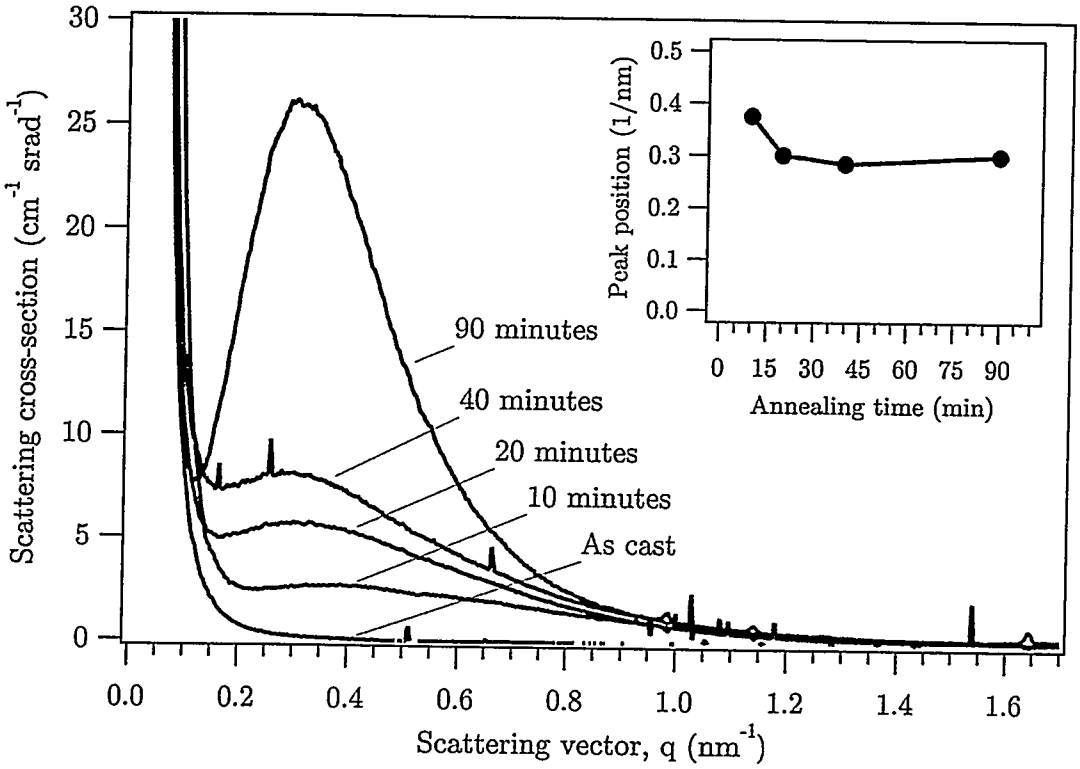
Scattering cross-section (cm^{-1} srad^{-1})
Scattering vector, q (nm^{-1})
90 minutes
40 minutes
20 minutes
10 minutes
As cast
Peak position (1/nm)
Annealing time (min)

Figure 3:

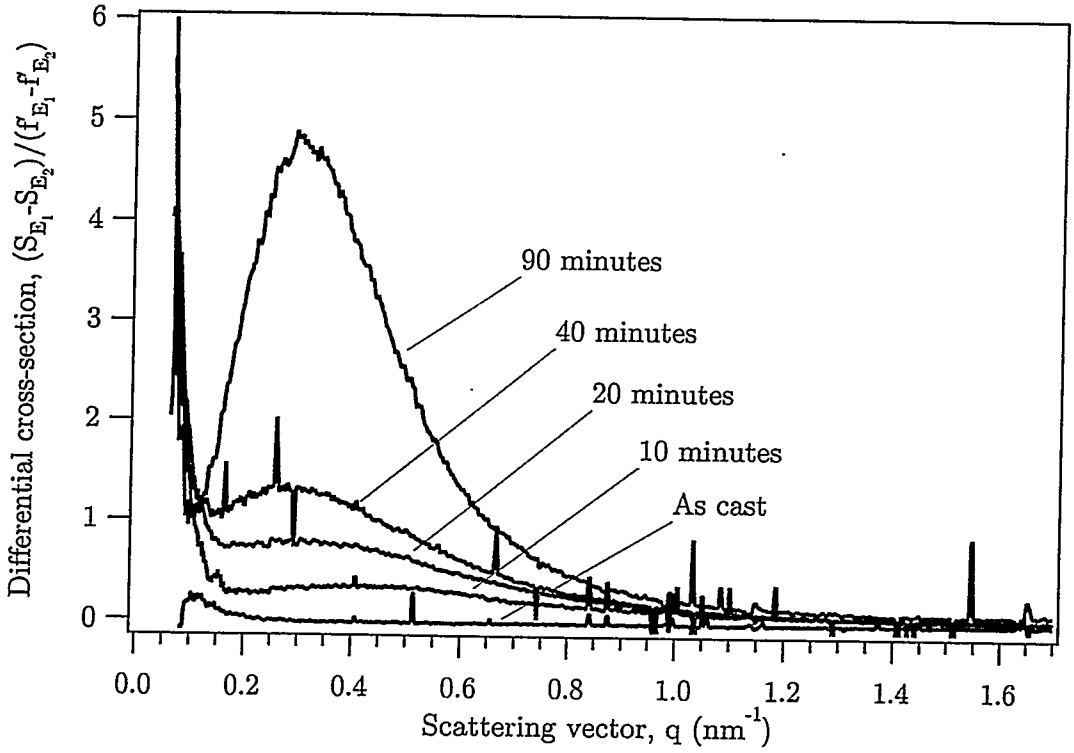
Differential cross-section, $(S_{E_1}-S_{E_2})/(f'_{E_1}-f'_{E_2})$
Scattering vector, q (nm^{-1})
90 minutes
40 minutes
20 minutes
10 minutes
As cast
0
1
2
3
4
5
6
0.0
0.2
0.4
0.6
0.8
1.0
1.2
1.4
1.6

Figure 4: